

## Research Article

# Relationship between Particle Size, Anti-Microbial Activity and Leachability of Copper Particles in Liquid Suspension and Compounded in Polypropylene

Saleh Alkarri<sup>1\*</sup> and Jérôme Vachon<sup>2</sup><sup>1</sup>School of Packaging, Michigan State University, 448 Wilson Road, East Lansing, MI 48824-1223, USA<sup>2</sup>SABIC T&I, Urmonderbaan 22, 6167 RD Geleen, P.O. Box 319, 6160 AH Geleen, Netherlands

## Abstract

Testing the antimicrobial efficiency of plastics with good precision and repeatability remains a challenge in the plastic industry, as commonly used standards can provide unreliable data. In this paper, we show that the “Bacterial Liquid Suspension Test” is a reliable method that allows for the measurement of antimicrobial activity of poor to very potent biocides. We used this technique to discriminate the performance of two Cu-based biocides, either in nanoparticle (NP) or macroparticle (MP) size, at three different loadings (0.02, 0.2 and 2 wt.%) in PP. With this technique, we also tested the antibacterial performance of PP as powders, pellets, and injection molded disks. As anticipated, the technique shows that both the increased loading and the smaller particle size showed higher antimicrobial activity than the larger particle size due to their increased surface area. Also, PP powders showed greater bacterial reduction than pellets and disks. While the PP with 2 wt.% Cu NPs showed the best antimicrobial performance, the detection of Cu at the surface (using SEM-EDX) and in the water leachate (using ICP-MS) were below the LODs, indicating their ability to kill bacteria.

## Introduction

After the COVID-19 pandemic, the global demand for materials with antimicrobial properties became more urgent [1]. The hygiene and safety of plastics, particularly those with surfaces that indicate the presence or growth of microbes (fungi, bacteria, and viruses), have become major concerns for consumers [2]. Warmth, humidity, and the presence of nutrients contribute to microbial growth, and plastics typically lack any defense against this [3]. Microorganisms adhering to artificial surfaces in damp conditions can survive and multiply. When the number of microbial cells increases, biofilm, a matrix of polysaccharides containing embedded cells, forms. Biofilms enable microbial survival in challenging environments and exhibit significantly reduced susceptibility, approximately 1000-fold, to most biocidal agents [4]. The toxins released by biofilms spread resilient bacterial strains that are resistant to multiple antimicrobial substances [5]. This creates the need to develop antimicrobial materials that “are capable of inhibiting or killing the microbes on their surface or within their surroundings” [6]. The use of

antimicrobial materials has been extensively investigated, and several approaches were developed, as shown by the plethora of patents and research studies [7]. When considering the production of antimicrobial polyolefins in particular, there are different ways to confer anti-microbial properties to the material: (i) direct incorporation of antimicrobial agents into polyolefin through a compounding step, (ii) applying an antimicrobial coating, and (iii) chemical incorporation using copolymerization or grafting (e.g. through reactive extrusion) to immobilize antimicrobial agents or to impart antimicrobial functionality onto polyolefin through either ionic or covalent linkages [8,9].

Heavy metal biocides, such as silver and copper nanoparticles (NPs), traditionally used as anti-microbial agents, can be readily integrated into polyolefin through extrusion techniques, potentially imparting effective antimicrobial properties to the materials with a short contact duration of several hours [10]. When exposed to moisture, an electromagnetic process leads to the release of silver ions, which infiltrate microbes and reduce their functionality and

## More Information

\*Address for correspondence: Saleh Alkarri, School of Packaging, Michigan State University, 448 Wilson Road, East Lansing, MI 48824-1223, USA, Email: [alkarris@msu.edu](mailto:alkarris@msu.edu)

 <https://orcid.org/0009-0003-3549-9585>

Submitted: May 22, 2024

Approved: May 28, 2024

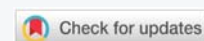
Published: May 29, 2024

How to cite this article: Alkarri S, Vachon J. Relationship between Particle Size, Anti-Microbial Activity and Leachability of Copper Particles in Liquid Suspension and Compounded in Polypropylene. *Ann Biomed Sci Eng.* 2024; 8: 021-031.

DOI: [10.29328/journal.abse.1001030](https://doi.org/10.29328/journal.abse.1001030)

Copyright license: © 2024 Alkarri S, et al. This is an open access article distributed under the Creative Commons Attribution License, which permits unrestricted use, distribution, and reproduction in any medium, provided the original work is properly cited.

Keywords: Antimicrobial activity; *E. coli* K-12 MG1655; Copper particles; Leachability; Compounding



ability to reproduce [11]. Therefore, their mode of action is through the process of leaching from the plastic to the microorganism. Some studies have shown that prolonged exposure to silver ions can negatively affect human health (skin discoloration, known as argyria, or eye discoloration, termed argyrosis, can occur; also, exposure to soluble silver compounds may cause liver and kidney damage and lead to irritation of the eyes, skin, respiratory system, and intestinal tract) [12]. Additionally, controlling the amount of silver waste disposed of in nature is a concern, especially in marine environments, where the release of silver was shown to be harmful to aquatic life [13]. The immobilization of silver onto carriers (ZnO, glass, zeolite) limits the release of silver into the environment; nevertheless, the European Chemicals Agency (ECHA) determined it could no longer approve these technologies for food contact applications [14]. Therefore, there is a need for more environmentally friendly and less toxic antimicrobial additives in plastics; the type of inorganic biocide, as well as its size and shape, is important. Copper exhibits antimicrobial properties, and, like silver, has been used to sterilize liquids or treat human wounds for centuries [15,16]. The mechanism of the biocidal action of Cu ions is complex since some copper ionic species can be formed (e.g.  $\text{Cu}^{2+}$  and  $\text{Cu}^+$ ). Additionally, Cu NPs can be oxidized to  $\text{CuO}$  or  $\text{Cu}_2\text{O}$ , and each of these different moieties can interact with a cell's vital functions [10]. In general,  $\text{Cu}^+$  is connected to the production of highly reactive substances like hydroxyl radicals, which disrupt the membrane's integrity and cause oxidative stress to the cell, while  $\text{Cu}^{2+}$  forms complexes with bacteria's functional groups (proteins, DNA, etc.), resulting in ion substitution and enzyme deactivation [17-19]. For most antimicrobial additives compounded into plastics, their migration properties and leachability propensity are crucial since the biocidal mechanism involves ions migrating from the plastic matrix to the surface and then to the microbe. Therefore, a key distinction is made when dealing with dry and humid surfaces as depicted in Figure 1.

Different factors affect bacterial survival on inanimate surfaces, and depending on the type of bacteria [20], their survival rate on dry surfaces can range from days to months [21]. This article particularly focuses on studying the influence of the particle size of copper (macro vs. nano with spherical particle shape) on antimicrobial properties using a specific antimicrobial testing procedure that allows for the constant renewal of bacterial cultures on the surface of neat PP disks and PP composites (powders, pellets, and disks). This procedure removes any misleading data caused by intrinsic wetting issues (hydrophobicity). The PP composites with spherical-shaped Cu-nanoparticles and spherical-shaped Cu-microparticles were processed at three different mixing ratios (0.02 wt.%, 0.2 wt.%, and 2 wt.%). The formation of PP composites was studied using SEM and EDX. The thermal characteristics were analyzed using DSC and TGA, and the leachability was characterized using ICP-MS for the composites of PP disks.

## Experimental

### Materials

Polypropylene homopolymer (PP 500 P grade) was procured from SABIC (Riyadh, Saudi Arabia) as a powder with the following properties: melting point: 230 °C, density: 0.905 g/cm<sup>3</sup>, and melt flow MFR = 3 g/10 min at 230°C / 2.16 kg; Mw ~ 300 kg/mol, isotacticity ~ 96%. Copper nanoparticles (purity: 99.99%) were obtained from Nanomaterial Powder (Istanbul, Turkey) as a dry powder with an average particle size of 570 nm. Copper microparticles (purity: 99.99%) were obtained from Sigma Aldrich (Missouri, USA) as a dry powder with an average particle size of 425 μm.

### Melt-compounding and injection molding of PP with antimicrobial agents

Physical mixing of the additive package with the PP resin was carried out for each formulation, ensuring enough homogeneity of the mixtures applied before the melt mixing. Extrusion was performed using a twin-screw extruder from Thermofisher (Process 11: D 11 mm, L/D 40). The operating conditions were kept the same for all experiments. The extruder temperature profile was set from 60 to 230 °C. The extruder screw rotation speed was kept at 223 rpm. The mixing ratios for both Cu-nanoparticles and Cu-microparticles were (i) 0.02 wt.%, (ii) 0.2 wt.%, and (iii) 2 wt.%. Extrusion compounding resulted in PP polymer pellets with the desired level of additives. The composite pellets were further processed to make a PP powder of both Cu-nanoparticles and Cu-microparticles composites at (i) 0.02 wt.%, (ii) 0.2 wt.%, and (iii) 2 wt.% using a lab scale pellets grinder model EBERBACH E3300.00, Mini Cutting Mill, MI, USA (Figure 2). Injection molding of the pellets was performed using a Babyplast 6/12 machine. The processing temperature was 230 °C, and the mold temperature was 60 °C using 5x5x0.32 cm molds. The neat PP and six compounded PPs were injection-molded into disks (the disk measured 25 millimeters in diameter and had a thickness of 1.55 millimeters). The disks were of a size that could be used in antimicrobial testing equipment. The untreated PP did not display antimicrobial activity; therefore, it was selected as a negative control sample.

### Antimicrobial testing method

The antimicrobial properties of the disks were assessed using *E. coli* K-12 MG1655 procured from the American Type Culture Collection in Manassas, VA. The stock culture was stored at -80 °C and streaked onto TSA plates from BBL/Difco in Sparks, MD, USA. After incubation at 37 °C for 24 hrs, a single colony was chosen and transferred to 5 mL of TSB, also from BBL/Difco, where it incubated at 37 °C for 18 hours. Following incubation, 1 mL of culture was centrifuged at 13,000 x g for 5 minutes using a Fisher Scientific accuSpin micro 17 R centrifuge, and the supernatant was disposed of. Through vortexing, the cells were then suspended in 1 mL of phosphate-buffered saline (PBS) from Crystalgen



Figure 1: The living mechanism of bacteria on dry and wet surfaces of PP composites.



Figure 2: Lab scale grinder.

in Commack, NY, USA. This cell suspension was transferred to a 15 mL tube, and 11.5 mL of PBS was added. Aliquots of this suspension were then exposed to different types of (i) antimicrobial particles (powders), (ii) neat PPs (powders, pellets, and disks), and (iii) composite PPs (powders, pellets, and disks) that contain antimicrobial additives.

Each single material (20 g of powders, 20 g of pellets, and 1 disk which weighed ~ 20 g) was individually positioned in a pod consisting of contact lens cases manufactured by Bosch + Lomb [22]. 1 mL of bacterial suspension was added to each pod containing a single type of material, including (i) anti-microbial particles (powders), (ii) neat PPs (powders,

pellets, and disks), and (iii) composite PPs (powders, pellets, and disks). Once each material was submerged in the culture broth, its pod was closed. Then, the pods were affixed onto a mini rotator (Benchmark Scientific, Roto Mini Plus R 2024, Sayreville, NJ, USA) and set to rotate at 20 rpm around the machine's horizontal axis, ensuring continuous agitation of the broth and facilitating liquid replenishment on the tested materials. At intervals of 0, 4, and 24 hrs, a 100  $\mu$ L sample of the bacterial suspension was extracted for 1:10 dilutions, plated in TSA, and subsequently incubated overnight at 37  $^{\circ}$ C. The number of colony-forming units (CFUs) was enumerated to assess cell viability.

### Experimental design

A 2x3x3 factorial experiment was used to assess the impact of the antimicrobial agents against *E. coli* K-12 MG1655 on the melt compounded PPs. The factorial experiments were performed as follows: antimicrobial particle size (570 nm and 425  $\mu$ m), antimicrobial agent concentration (0.02 wt.%, 0.2 wt.%, and 2 wt.%), and melt-compounded composite shape (powders, pellets, and disks).

### Statistical analysis

Each experiment was conducted with three separate biological replicates. Variations in the means of *E. coli* K-12 MG1655 cell density resulting from direct exposure to the following were analyzed: (1) pristine PP disk (serving as the negative control), and (2) PP composites containing antimicrobial agents were assessed at 0, 4, and 24 hrs using Tukey's honest significant difference test and Student's *t*-test

at a confidence level of 96% ( $p \leq 0.05$ ). Interactions among the particle sizes of antimicrobial agents (nano and micro-size), mixing ratio of the antimicrobial agents with PP (0.02 wt.%, 0.2 wt.%, and 2 wt.%), composite sample shape (powders, pellets, and disks), and the antimicrobial activity were evaluated using four-way analysis of variance (ANOVA) with Origin 2022b software (vs. 9.9.5.167; OriginLab Corporation, Massachusetts, USA).

### Sample characterization

**Bacteria in aqueous suspension test:** The antimicrobial activity of the agents (pure particles without polymer) was tested in aqueous bacterial suspension, and the reduction in *E. coli* K-12 MG1655 cell density was observed at two time intervals (4 and 24 hrs). 18 mg of the antimicrobial particles (powders) were added to 1 mL of *E. coli* K-12 MG1655 in bacterial aqueous solution (liquid) using a microcentrifuge tube and rotated at 20 rpm using a sample mini rotator. 100  $\mu$ L of the solution was extracted for plating in TSA at 4 and 24 hrs.

### Antimicrobial test for neat and composite PPs

The antimicrobial activity of neat PP and composite PPs were tested in three different shapes (powders, pellets, and disks), Three levels of concentration in PPs (0.02 wt.%, 0.2 wt.%, and 2 wt.%), and two sizes of Cu anti-microbial agents with spherical shapes (nanoparticles and microparticles) were studied.

### Scanning Electronic Microscopy (SEM) and Energy Dispersive X-ray (EDX) preparation methods

The antimicrobial particles (pure powders of Cu-nanoparticles or Cu-microparticles), along with the compounded and injection molded PP disks with (0.02 wt.%, 0.2 wt.% and 2 wt.% of either Cu-nanoparticles or Cu-microparticles) were characterized by SEM using a JEOL 7500F field emission emitter (JEOL Ltd., Tokyo, Japan), and by energy dispersive X-ray EDX analysis using an Oxford Instruments Aztec system (Oxford Instruments, High Wycomb, Bucks, England). Samples were prepared for analysis by mounting them on aluminum stubs using the Epoxy glue, System Three Quick Cure 5 (System Three Resins, Inc., Auburn, WA). Each mounted sample was coated with ( $\sim 2.7$  nm thickness) iridium in a Quorum Technologies/Electron Microscopy Sciences Q150T turbo-pumped sputter coater (Quorum Technologies, Laughton, East Sussex, England BN8 6BN) and purged with argon gas.

### Differential Scanning Calorimetry (DSC)

The melting point and crystallinity temperature of PP samples were calculated using a TA Instrument Model Q100 system with nitrogen flow set at 70 mL min<sup>-1</sup>. Samples were analyzed within a temperature range of -20 to 250 °C at a rate of 10 °C.min<sup>-1</sup>, with a sixty-second pause to eliminate prior thermal history. Additionally, samples were cooled to -20

°C at 10 °C.min<sup>-1</sup> and reheated to 250 °C at the same rate to record thermal responses. Each sample underwent at least three replications. The degree of crystallinity was determined based on heat of fusion values obtained during an additional heating run and assessed using Equation (1).

$$X_c (\%) = \left[ \frac{\Delta H_c}{\Delta H_0 \cdot W} \right] \times 100 \quad (1)$$

In Equation (1),  $X_c$  represents the crystallinity of PP samples,  $\Delta H_c$  denotes the heat of fusion  $\Delta H_f$ , stands for the enthalpy of fusion for 100% crystalline PP [209 J/g] [23] and  $W$  indicates the fraction (weight) of PP in the composite.

**Thermal Gravimetric Analysis (TGA):** Thermal characterization of the PP samples was conducted with a TA Instrument (Model Q50, thermogravimetric analysis (TGA) technique). A sample weighing ( $8 \pm 2$  mg) was placed into an aluminum pan, and the temperature was gradually increased from (20 to 600 °C) at a heating rate of (10 °C/min) within a nitrogen atmosphere flowing at a rate of (40 mL/min).

**Cu leachability measurements of pp composites:** The leachability of the compounded polypropylene (disks) with Cu-nanoparticles and Cu-macroparticles at the highest level of dosing (2 wt.%) was analyzed using inductively coupled plasma mass spectrometry (ICP-MS). The tests were performed according to the procedure illustrated in Figure 3. A razor was used to cut the disks into small pieces. A ratio of 200 mg of sample per 0.5 mL of water was used for each sample, and the amount of copper leached was measured at two intervals (4 and 24 hrs) at room temperature (20 °C). Water samples were 100 - 5000 times diluted in 5% nitric acid (trace metal grade). The elements in the water samples were quantified by ICP-MS using a multi-element calibration set from Inorganic Ventures and an Agilent 8900 ICP-MS system.

## Results and discussion

### Bacterial liquid suspension test

We first assessed the antimicrobial efficacy of the two copper additives themselves, before compounding them in PP using the liquid suspension test. The amount of additive used in the test corresponds to the total amount dosed in the PP materials when using 2 wt.% loading. We assessed the *E. coli* bacterial reduction at two different time intervals (4 and 24 hrs). Both nano-Cu and macro-Cu resulted in significant bacterial reductions. While after 4 hrs, there was no strong distinction between the two forms, after 24 hrs, the nano-Cu gave a slightly better result with a log 8 reduction vs. a log 7 for the macro-Cu (Figure 4). This first confirms the slight superiority of the antimicrobial ability of nanoparticles compared to macroparticles.

### Anti-microbial Test for Neat and Composite PP samples

In the first set of experiments, we measured the effect of the

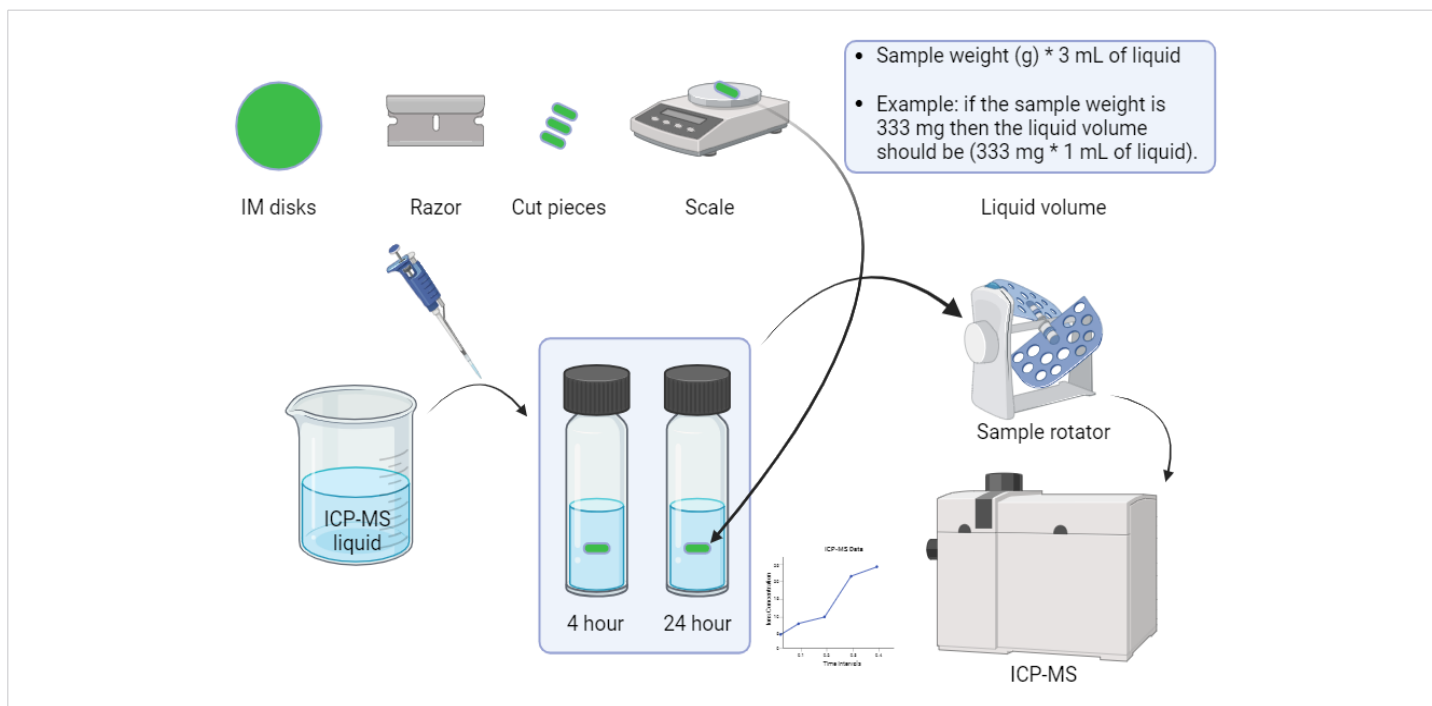


Figure 3: Illustration of ICP-MS experimental procedure.

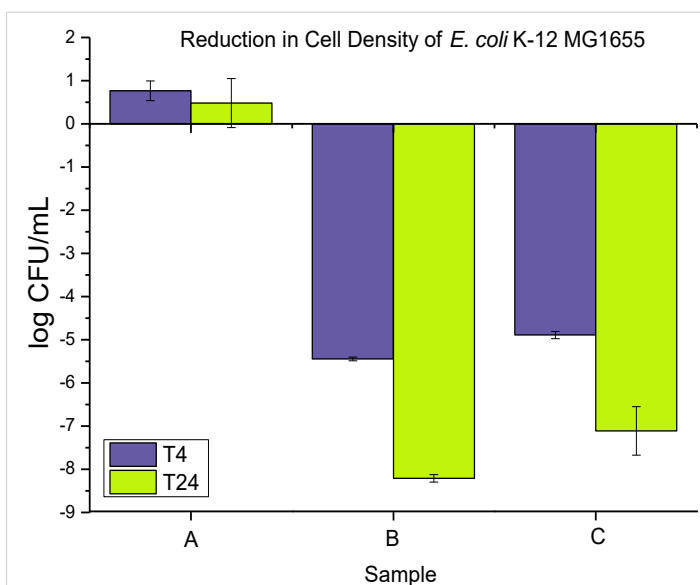


Figure 4: Represent the anti-microbial activity of (A) neat *E. coli* bacterial cultures, (B) Cu-nanoparticles, and (C) Cu-microparticles.

two additives compounded at (2 wt.%) in PP and tested them in three different shapes (powders, pellets, and disks). First, as a control, we confirmed that the untreated PP disk showed no antimicrobial activity; in fact, a slight growth of *E. coli* was observed over 24 hrs (Figure 5A). As expected, the antibacterial effect observed was slightly lower in compounded PP vs. the neat additives, since only a small amount of Cu leached into the liquid suspension. Again, the best results were obtained when using nano-Cu with a bacterial reduction up to log 5.5 in PP powder after 24 hrs. The sample form also had an influence, and better results were obtained for the PP powders, which have a larger surface area than the pellets and disks. These

two parameters (nano vs. macro and powders vs. pellets vs. disks) are, however, only visible after 24 hrs, as after 4 hrs of experiments, all results were fairly comparable. This could be explained by the very high loading of the copper additive used here, which was potentially present in enough quantities on the surface of the PP at the start of the experiment to already have a significant biocidal effect. After 24 hrs, a migration of the Cu through the PP matrix could potentially occur where the shape of the PP and the size of the Cu would influence such a phenomenon.

*The antimicrobial activity of neat PP and 0.02 wt.% nanoparticles and microparticles composites is presented in (Figure 5) as (i) powders, (ii) pellets, and (iii) disks at T4 and T24.*

*Antimicrobial activity of neat PP, and 0.2 wt.% nanoparticle and microparticle composites is presented in Figure 6 as (i) powders, (ii) pellets, and (iii) disks at T4 and T24.*

When reducing the loading in PP to 0.2 wt.%, the bacterial reduction was reduced with only up to log 4 in the best case (PP powders with nano-Cu). Similar observations can be made compared to the 2 wt.% experiments in terms of the effect of nano vs. macro and PP form. However, in that set of experiments, the PP pellets proved to be far superior to the disks for both T4 and T24. A reduced loading means less additive on the surface, which can exacerbate the effect of the surface area to an even higher degree than at higher Cu loading. This hypothesis is further validated when using a very low loading of Cu (0.02 wt.%). In this case, we can expect that very little amount of Cu is present initially on the surface, which leads to very low bacterial reduction at T4, barely reaching log 2 in the best cases.

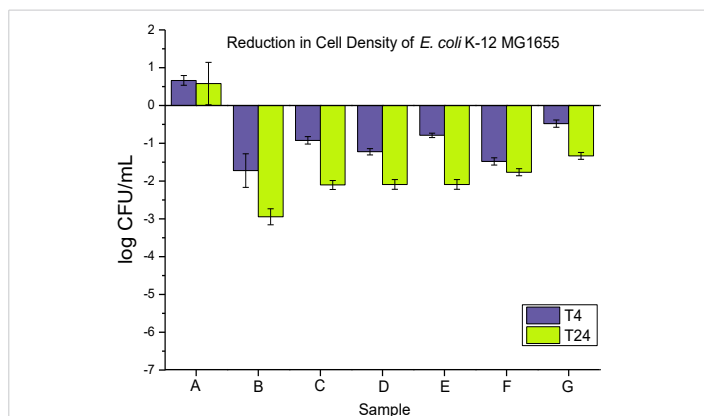


**Figure 5:** Represents the anti-microbial activity of (A) neat PP, and (B) PP powders compounded with 0.02 wt.% NPs, (C) PP powders compounded with 0.02 wt.% MPs, (D) PP pellets compounded with 0.02 wt.% NPs, (E) PP pellets compounded with 0.02 wt.% MPs, (F) PP disks compounded with 0.02 wt.% NPs, and (G) PP disks compounded with 0.02 wt.% MPs.

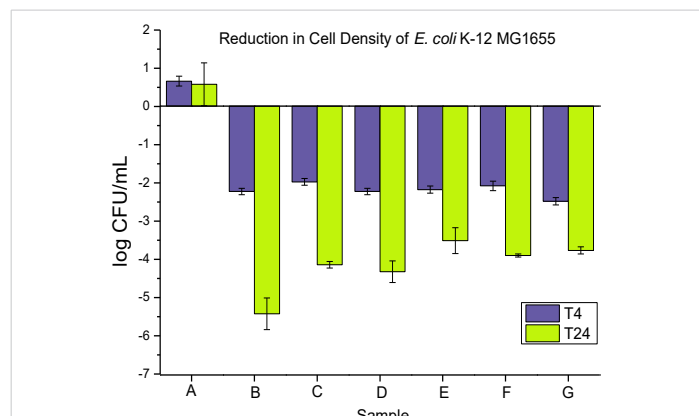


**Figure 7:** Represents the anti-microbial activity of (A) neat PP, (B) PP powders compounded with 2 wt.% NPs, (C) PP powders compounded with 2 wt.% MPs, (D) PP pellets compounded with 2 wt.% NPs, (E) PP pellets compounded with 2 wt.% MPs, (F) PP disks compounded with 2 wt.% NPs, and (G) PP disks compounded with 2 wt.% MPs.

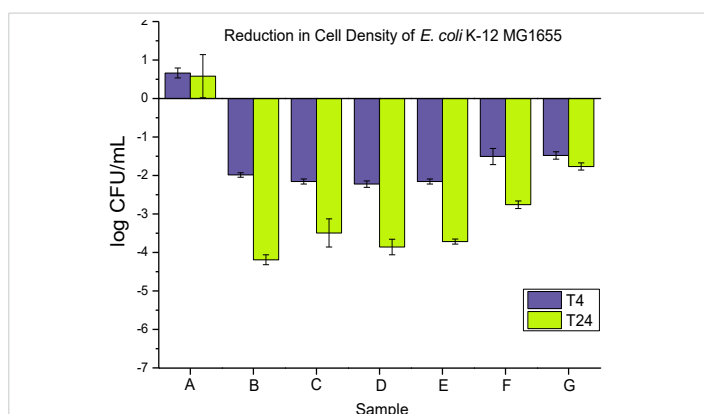


**Figure 6:** Represents the anti-microbial activity of (A) neat PP, (B) PP powders compounded with 2 wt.% NPs, (C) PP powders compounded with 2 wt.% MPs, (D) PP pellets compounded with 2 wt.% NPs, (E) PP pellets compounded with 2 wt.% MPs, (F) PP pellets compounded with 2 wt.% MPs, (F) PP disks compounded with 2 wt.% NPs, and (G) PP disks compounded with 2 wt.% MPs.

Antimicrobial activity of neat PP, and 2 wt.% nanoparticle and microparticle composites is presented in Figure 7 as (i) powders, (ii) pellets, and (iii) disks at T4 and T24.

Overall, we showed that the liquid suspension test proved to be a very effective tool for assessing the antimicrobial efficiency of either additives alone or compounded articles. It can discriminate the effect of the morphology of additives (nano vs. macro) and the surface area of the articles. The method is very robust with typically small standard variation and a high log CFU scale, which allows measuring from poor to very potent biocides. This is not always the case in other methods such as the ISO 22196:2011 (and similar methods such as JIS Z 2801), which is the most widely used standard for measuring antibacterial activity on plastic surfaces. While this standard is affordable and easy to use, the results of this technique have varied greatly among different laboratories [24].

### Scanning Electronic Microscopy (SEM)

#### SEM of dry powder of Cu nanoparticles and Cu

**microparticles:** The SEM images of dry powder of Cu nanoparticles and Cu microparticles are presented in Figures 8,9, respectively.

In both cases, the Cu NPs and Cu MPs crystals have a reddish-brown color. The SEM images of the Cu in Figure 8 show the particles were spherical. The particles were about 344-865 nm, and the average particle size was approximately 570 nm. The spherical particles seem to have clustered together, and in certain instances, there appear to be crystal formations growing over them. Similarly, the Cu MPs particles are also spherical (Figure 9) and sometimes present as agglomerates. In this case, the particle size ranged from 260 to 540  $\mu\text{m}$ , with an average particle size of about 420  $\mu\text{m}$ .

**SEM and EDX of outer surface view of PP composites with 2 wt.% Cu NPs:** The results of the SEM and EDX outer surface view of PP composites with 2 wt.% Cu NPs are presented in Figure 10.

**SEM and EDX of the cross-sectional view of PP composites with 2 wt.% Cu NPs:** The results of the SEM and EDX cross-sectional view of PP composites with 2 wt.% Cu NPs are presented in Figure 11.

**SEM and EDX of outer surface view of PP composites with 2 wt.% Cu MPs:** The results of the SEM and EDX outer surface view of PP composites with 2 wt.% Cu MPs are presented in Figure 12.

**SEM and EDX of the cross-sectional view of PP composites with 2 wt.% Cu MPs:** The results of the SEM and EDX cross-sectional view of PP composites with 2 wt.% Cu MPs are presented in Figure 13.

We further performed SEM-EDX on PP disk samples to better understand the distribution of Cu particles in the composites. We only measured samples containing 2 wt.% of Cu, as the sensitivity of the EDX technique is rather poor, with a detection limit of elements at about a 1000 ppm level [25].

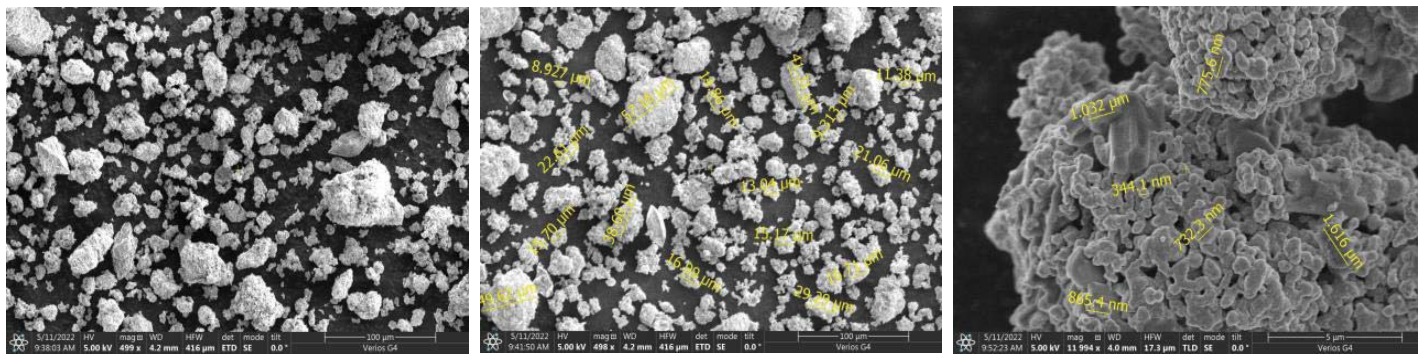


Figure 8: Shows the SEM images of pure Cu Nanoparticles.

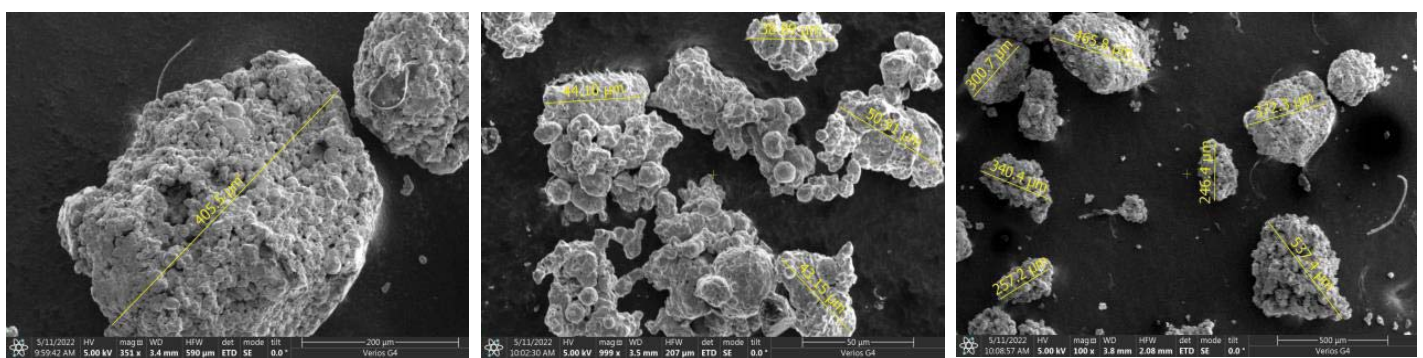


Figure 9: Shows the SEM images of pure Cu Microparticles.

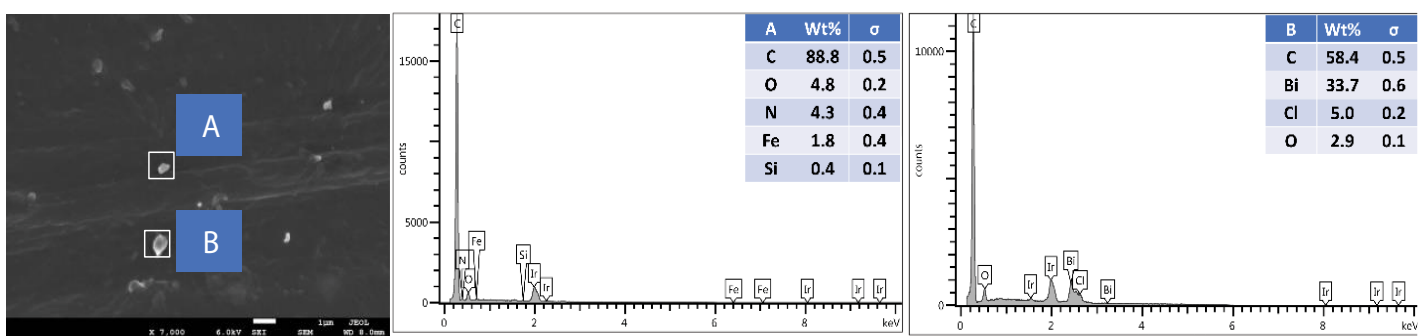


Figure 10: Shows the SEM and EDX of the outer surface view of PP composites with 2 wt.% Cu NPs.

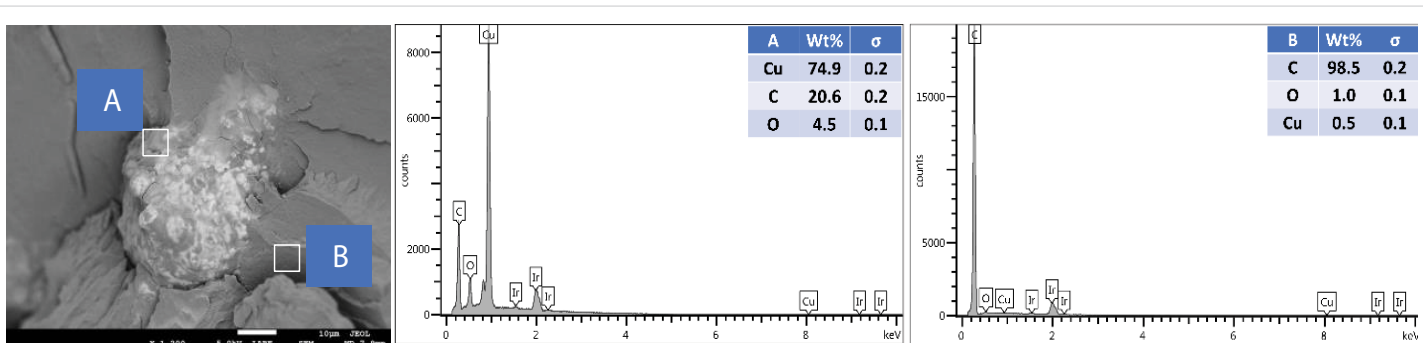


Figure 11: Shows the SEM and EDX of a cross-sectional view of PP composites with 2 wt.% Cu NPs.

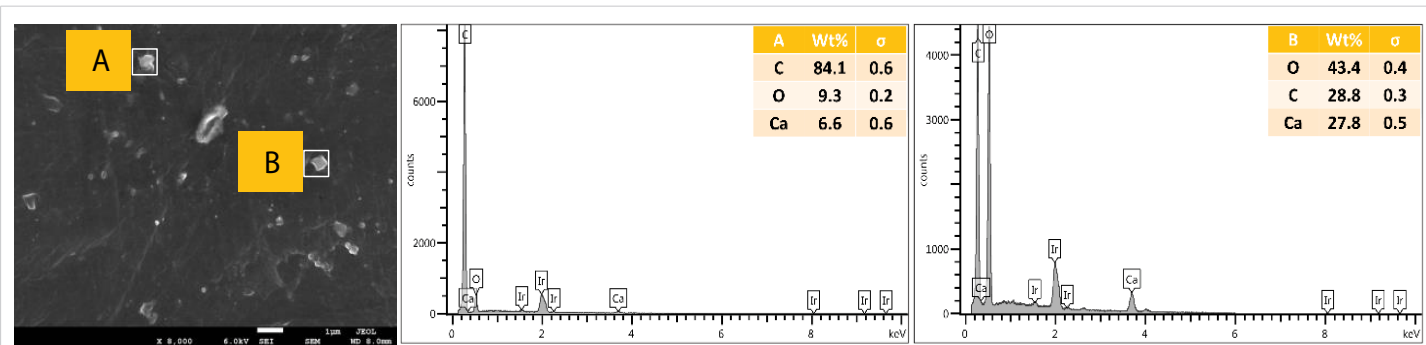


Figure 12: Shows the SEM and EDX of the outer surface view of PP composites with 2 wt.% Cu MPs.

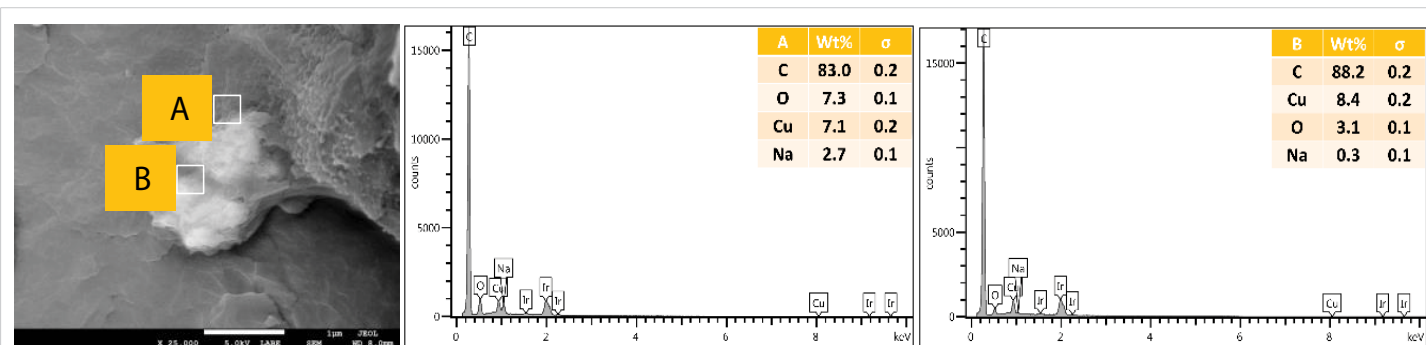


Figure 13: Shows the SEM and EDX of the cross-sectional view of PP composites with 2 wt.% Cu MPs.

The penetration depth is at the micron level, which means there are overlapping signals from the micron level with the surface. We performed the analysis of both the disk surfaces as well as the cross-section to compare the distribution of the Cu within the bulk and the surface of the samples. From the SEM images, it was observed that there were a few particles and agglomerates of Cu present, especially for the MPs. For both Cu NPs and MPs, the EDX could not catch the signal of the Cu, meaning that the Cu concentration is below the detection limit of EDX (Figures 10,12). In contrast, the EDX detected Cu within the bulk of the PP composites, yet at a very low level and irrespective of where the signal was recorded (A and B zones, Figures 11,13), probably due to the detection depth of the technique. Overall, this showed that only a limited amount of Cu is present at and near the surface, which accounts for the antimicrobial performance and the fact that most of the Cu is located within the bulk of the PP matrix, acting potentially as a reservoir for antimicrobial agents.

### Differential scanning calorimetry (DSC)

The influence of the antimicrobial additives (loading and size) on the thermal properties of the PP composites was measured by DSC (Figure 14). Overall, minor differences between the PP samples were observed in terms of crystallization temperature ( $T_c$ ) and melting temperature ( $T_m$ ) as listed in Table 1. In all cases,  $T_m$  was barely affected, while minor changes were observed on  $T_c$  at 2 wt.% loading of Cu

NPs and Cu MPs (up to 2 °C difference compared to the neat PP sample). Only samples with 2 wt.% of Cu NPs had a noticeable increase in the crystallization degree (from ~40 to ~43%), which overall indicates a slight nucleating aid behavior.

The percentage of crystallinity in various melt-compounded and injection-molded PP samples is displayed in Table 1.

### Thermal Gravimetric Analysis (TGA)

The TGA analysis of neat PP and PP composites with the antimicrobial agents was performed to determine their thermostability as shown in Figure 15.

The 5% weight loss for melt-compounded and injection molded PP disks loaded with Cu NPs at (0.02, 0.2, and 2 wt.%) occurred at ( $336.39 \pm 0.92$  °C,  $340.90 \pm 0.73$  °C, and  $343.16 \pm 0.39$  °C, respectively), and for Cu MPs occurred at ( $345.28 \pm 0.88$  °C,  $350.68 \pm 0.47$  °C, and  $352.82 \pm 0.67$  °C, respectively) as presented in Table 2. Overall, both the Cu NPs and Cu MPs increased the thermal stability of the PP samples at a higher loading rate, except for Cu NPs at 0.02 wt.% loading.

### Copper leachability of the disks

The leachability of copper into water from the PP disks was measured using the highest Cu loading, as we expected a rather slow phenomenon. The Cu content was measured in the leachate by ICP-MS after 4 and 24 hrs contact time of the PP disk composites (cut into small pieces) with water. We



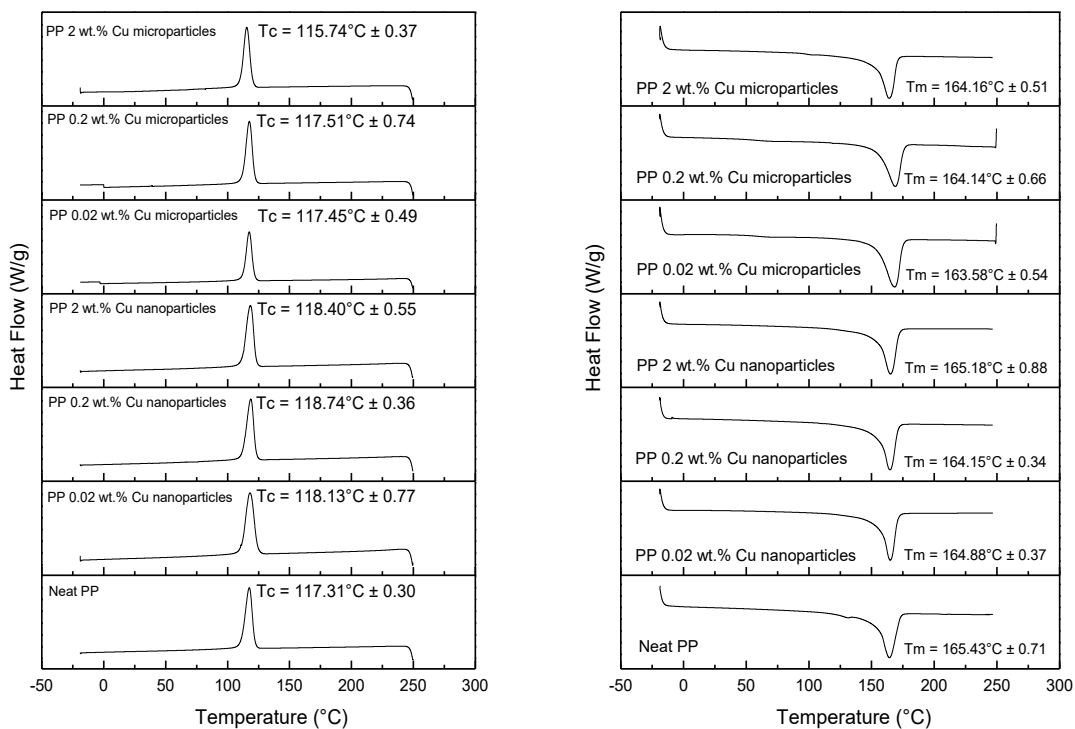


Figure 14:  $T_c$  (left) and  $T_m$  (right) values were obtained from the DSC data for various samples.

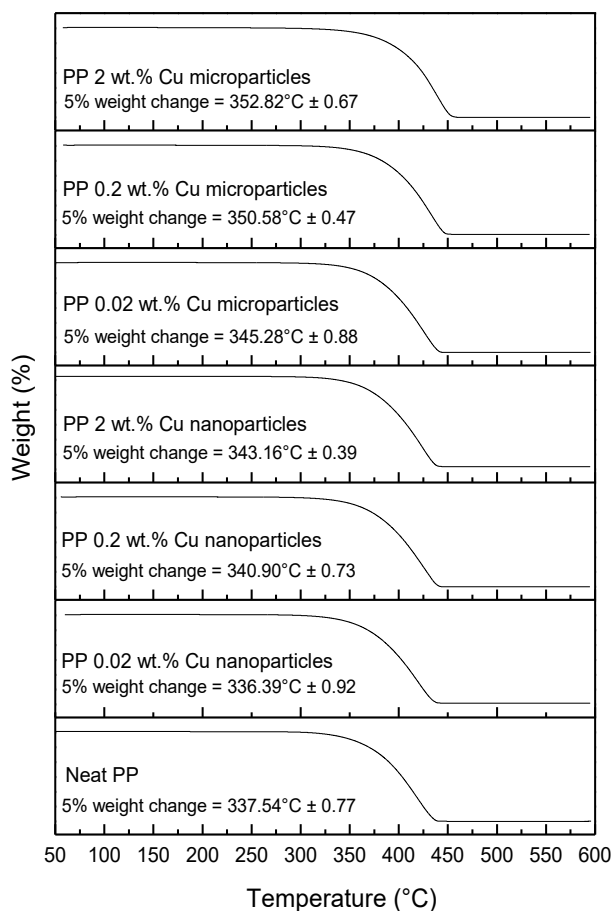


Figure 15: Shows the TGA characterization of neat PP, and various PP composites.

**Table 1:** The degree of crystallinity in PP samples was determined through DSC measurements.

Samples	$\Delta H_m$ (J/g)	$T_m$ (°C)	$T_c$ (°C)	Crystallinity (%)
Neat PP	83.59 ± 1.27	165.43 ± 0.71	117.31 ± 0.30	39.99 ± 0.61
PP 0.02 wt% Cu nanoparticles	76.11 ± 1.64	164.88 ± 0.37	118.13 ± 0.77	36.42 ± 0.73
PP 0.20 wt% Cu nanoparticles	84.15 ± 1.43	164.15 ± 0.34	118.74 ± 0.36	40.26 ± 5.73
PP 2.00 wt% Cu nanoparticles	90.23 ± 2.00	165.18 ± 0.88	118.40 ± 0.55	43.17 ± 2.17
PP 0.02 wt% Cu microparticles	74.43 ± 5.47	163.58 ± 0.54	117.45 ± 0.49	35.61 ± 2.74
PP 0.20 wt% Cu microparticles	81.25 ± 7.54	164.14 ± 0.66	117.51 ± 0.74	38.88 ± 1.64
PP 2.00 wt% Cu microparticles	84.48 ± 3.45	164.16 ± 0.51	115.47 ± 0.37	40.42 ± 3.64

**Table 2:** 5% weight change of PP samples obtained from TGA measurements.

Sample	5 % weight change occurred at temperature (°C)
Neat PP	337.54 ± 0.77
PP 0.02 wt.% Cu nanoparticles	336.39 ± 0.92
PP 0.20 wt.% Cu nanoparticles	340.90 ± 0.73
PP 2.00 wt.% Cu nanoparticles	343.16 ± 0.39
PP 0.02 wt.% Cu microparticles	345.28 ± 0.88
PP 0.20 wt.% Cu microparticles	350.68 ± 0.47
PP 2.00 wt.% Cu microparticles	352.82 ± 0.67

**Table 3:** Amount of Cu leaching out in water vs. amount of Cu initially detected in PP disks (2 wt.%).

Sample	4 hours	24 hours
PP Cu NPs (2 wt.%)	< 12 ppb	< 12 ppb
PP Cu MPs (2 wt.%)	187 ppb	963 ppb

calculated the amount of Cu lost from the initial amount of Cu in the PP (2 wt.%). In this technique, based on the limit of detection of Cu by ICP-MS (0.1 mg/kg), we calculated a LOD of Cu leached vs. Cu initially present in PP at ~ 12 ppb level. As seen in Table 3, no Cu leaching occurred (below LOD) in PP containing Cu NPs. A slight Cu loss was, however, noticed with Cu MPs, barely reaching 1 ppm after 24 hrs, indicating that the leaching of Cu occurred rather slowly at room temperature. The antimicrobial results obtained with both samples indicated that the Cu NPs do not necessarily work by leaching copper into water and that other surface mechanisms should occur.

## Conclusion

The “Bacterial Liquid Suspension Test” was successfully used to discriminate the biocidal performance of Cu-based additives in PP. Using this technique, the log reduction of the bacterial count of *E. Coli* was measured after 4 and 24 hrs for PP composites where the type of Cu (NPs or MPs), its loading level in PP (0.02, 0.2 and 2 wt.%), and the shape of PP (powders, pellets, or molded disks) were varied. As anticipated, the technique shows that both the increased loading and the smaller particle size demonstrated higher antimicrobial activity compared to the larger particle size as a result of the increased surface area. Also, PP powder showed a higher bacterial reduction compared to pellets and disks. While the PP with 2 wt.% Cu NPs showed the best antimicrobial performance, the detection of Cu at the surface (using SEM-EDX) and in the water leachate (using ICP-MS) were below the LODs, indicating how effective they are against bacteria.

## Acknowledgment

Saleh Alkarri is grateful to SABIC Company which has generously funded his doctoral studies as well as all of his research needs at Michigan State University. We also would like to express our deepest gratitude to *Maria Soliman* from Sabic T&I for her commitment to proofreading this article.

## Author contributions

S.A. led all the processing, performed all the required characterization, and wrote the manuscript. J.V. conducted the ICP-MS and proofread the manuscript.

## References

- Ipek C, Gümüş H, Şimşek M, Tosun M. DFT and Molecular Docking Study of 1-(2'-Thiophen)-2-propen-1-one-3-(2,3,5-trichlorophenyl) (TTCP) Molecule as Antiviral to Covid-19 Main Protease. Arab J Sci Eng. 2023;48(1):1031-1040. doi: 10.1007/s13369-022-07293-4. Epub 2022 Oct 27. PMID: 36321067; PMCID: PMC9612599.
- Alkarri S. Developing Methods for Incorporating Antimicrobial Biocidal Nanoparticles in Thermoplastics. Michigan State University, 2023. <https://www.proquest.com/openview/3d3600d8ed0e1614fa1c801e2fd9dc3/1?pq-origsite=gscholar&cbl=18750&diss=y>
- Simmons JJP, Composites P. The why, what and wherefore of antimicrobial systems. 2003; 11(2):101-113.
- Kostakioti M, Hadjifrangiskou M, Hultgren SJ. Bacterial biofilms: development, dispersal, and therapeutic strategies in the dawn of the postantibiotic era. Cold Spring Harb Perspect Med. 2013 Apr 1;3(4):a010306. doi: 10.1101/cshperspect.a010306. PMID: 23545571; PMCID: PMC3683961.
- Douterelo I, Jackson M, Solomon C, Boxall J. Microbial analysis of in situ biofilm formation in drinking water distribution systems: implications for monitoring and control of drinking water quality. Appl Microbiol Biotechnol. 2016 Apr;100(7):3301-11. doi: 10.1007/s00253-015-7155-3. Epub 2015 Dec 5. PMID: 26637423; PMCID: PMC4786615.
- Jain A, Duvvuri LS, Farah S, Beyth N, Domb AJ, Khan W. Antimicrobial polymers. Adv Healthc Mater. 2014 Dec;3(12):1969-85. doi: 10.1002/adhm.201400418. Epub 2014 Nov 19. PMID: 25408272.
- Mahira S, Jain A, Khan W, Domb AJ. Antimicrobial materials—An overview. 2019. <https://doi.org/10.1039/9781788012638-00001>
- Siedenbiedel F, Tiller JCJP. Antimicrobial polymers in solution and on surfaces: overview and functional principles. 2012; 4(1):46-71.
- Santos MRE, Fonseca AC, Mendonça PV, Branco R, Serra AC, Morais PV, Coelho JFJ. Recent Developments in Antimicrobial Polymers: A Review. Materials (Basel). 2016 Jul 20;9(7):599. doi: 10.3390/ma9070599. PMID: 28773721; PMCID: PMC5456892.
- Palza H. Antimicrobial polymers with metal nanoparticles. Int J Mol Sci. 2015 Jan 19;16(1):2099-116. doi: 10.3390/ijms16012099. PMID: 25607734; PMCID: PMC4307351.
- Zapata PA, Tamayo L, Páez M, Cerda E, Azócar I, Rabagliati FM.

- Nanocomposites based on polyethylene and nanosilver particles produced by metallocenic "in situ" polymerization: synthesis, characterization, and antimicrobial behavior. 2011; 47(8):1541-1549. <https://doi.org/10.1016/j.eurpolymj.2011.05.008>
12. Raloff JJ. Forest invades tundra and the new tenants could aggravate global warming. 2008; 174(1):26-29.
  13. Prabhu S, Poulouse EK. Silver nanoparticles: mechanism of antimicrobial action, synthesis, medical applications, and toxicity effects. 2012; 2:1-10. <https://doi.org/10.1186/2228-5326-2-32>
  14. Alkarri S, Bin Saad H, Soliman M. On Antimicrobial Polymers: Development, Mechanism of Action, International Testing Procedures, and Applications. *Polymers (Basel)*. 2024 Mar 11;16(6):771. doi: 10.3390/polym16060771. PMID: 38543377; PMCID: PMC10975620.
  15. Delgado K, Quijada R, Palma R, Palza H. Polypropylene with embedded copper metal or copper oxide nanoparticles as a novel plastic antimicrobial agent. *Lett Appl Microbiol*. 2011 Jul;53(1):50-4. doi: 10.1111/j.1472-765X.2011.03069.x. Epub 2011 May 23. PMID: 21535046.
  16. De Vietro N, Conte A, Incoronato AL, Del Nobile MA, Fracassi F. Aerosol-assisted low-pressure plasma deposition of antimicrobial hybrid organic-inorganic Cu-composite thin films for food packaging applications. 2017; 41:130-134. <https://doi.org/10.1016/j.ifset.2017.02.010>
  17. Tamayo L, Azócar M, Kogan M, Riveros A, Páez M. Copper-polymer nanocomposites: An excellent and cost-effective biocide for use on antibacterial surfaces. *Mater Sci Eng C Mater Biol Appl*. 2016 Dec 1;69:1391-409. doi: 10.1016/j.msec.2016.08.041. Epub 2016 Aug 15. PMID: 27612841.
  18. Palza H, Quijada R, Delgado K. Antimicrobial polymer composites with copper micro-and nanoparticles: Effect of particle size and polymer matrix. 2015; 30(4):366-380.
  19. Faúndez G, Troncoso M, Navarrete P, Figueroa G. Antimicrobial activity of copper surfaces against suspensions of *Salmonella enterica* and *Campylobacter jejuni*. *BMC Microbiol*. 2004 Apr 30;4:19. doi: 10.1186/1471-2180-4-19. PMID: 15119960; PMCID: PMC411034.
  20. Hanczvikkell A, Tóth Á. Quantitative study about the role of environmental conditions in the survival capability of multidrug-resistant bacteria. *J Infect Public Health*. 2018 Nov-Dec;11(6):801-806. doi: 10.1016/j.jiph.2018.05.001. Epub 2018 May 18. PMID: 29784578.
  21. Kramer A, Schwebke I, Kampf G. How long do nosocomial pathogens persist on inanimate surfaces? A systematic review. *BMC Infect Dis*. 2006 Aug 16;6:130. doi: 10.1186/1471-2334-6-130. PMID: 16914034; PMCID: PMC1564025.
  22. Alkarri S, Sharma D, Bergholz TM, Rabnawaz M. Fabrication methodologies for antimicrobial polypropylene surfaces with leachable and nonleachable antimicrobial agents. 2023; 141(1).
  23. Brandrup J, Immergut EH, Grulke EA, Abe A, Bloch DR. *Polymer Handbook*. Wiley New York: 1999; 89. [http://nguyen.hong.hai.free.fr/EBOOKS/SCIENCE%20AND%20ENGINEERING/MECANIQUE/MATERIAUX/COMPOSITES/Polymer\\_Handbook/66286\\_fm.pdf](http://nguyen.hong.hai.free.fr/EBOOKS/SCIENCE%20AND%20ENGINEERING/MECANIQUE/MATERIAUX/COMPOSITES/Polymer_Handbook/66286_fm.pdf)
  24. Wiegand C, Völpel A, Ewald A, Remesch M, Kuever J, Bauer J, Griesheim S, Hauser C, Thielmann J, Tonndorf-Martini S, Sigusch BW, Weisser J, Wyrwa R, Elsner P, Hipler UC, Roth M, Dewald C, Lüdecke-Beyer C, Bossert J. Critical physiological factors influencing the outcome of antimicrobial testing according to ISO 22196 / JIS Z 2801. *PLoS One*. 2018 Mar 20;13(3):e0194339. doi: 10.1371/journal.pone.0194339. PMID: 29558480; PMCID: PMC5860763.
  25. Williams DB, Carter CB. Imaging strain fields. [Journal Abbreviation]. 2009; 441-461. [https://doi.org/10.1007/978-0-387-76501-3\\_26](https://doi.org/10.1007/978-0-387-76501-3_26)